Acta Pharmacologica Sinica (2013) 34: 137–145
 1671-4083/13 $32.00
www.nature.com/aps

Original Article

Astragalus polysaccharide stimulates glucose uptake in L6 myotubes through AMPK activation and AS160/TBC1D4 phosphorylation

Jian LIU[1], Jing-fang ZHANG[2], Jin-zhi LU[1], De-ling ZHANG[1], Ke LI[1], Ke SU[1], Jing WANG[1], Ye-min ZHANG[1], Nian WANG[1], Si-tu YANG[1], Lang BU[1], Jing-ping OU-YANG[1, *]

[1]*Department of Pathophysiology, School of Basic Medical Sciences, Wuhan University, Hubei Provincial Key Laboratory of Allergy and Immune-Related Diseases, Wuhan 430071, China;* [2]*Medical College, Jingchu University of Technology, Jingmen 448000, China*

Aim: To establish the mechanism responsible for the stimulation of glucose uptake by Astragalus polysaccharide (APS), extracted from *Astragalus membranaceus* Bunge, in L6 myotubes *in vitro*.
Methods: APS-stimulated glucose uptake in L6 myotubes was measured using the 2-deoxy-[^{3}H]-D-glucose method. The adenine nucleotide contents in the cells were measured by HPLC. The phosphorylation of AMP-activated protein kinase (AMPK) and Akt substrate of 160 kDa (AS160) was examined using Western blot analysis. The cells transfected with 4P mutant AS160 (AS160-4P) were constructed using gene transfer approach.
Results: Treatment of L6 myotubes with APS (100−1600 μg/mL) significantly increased glucose uptake in time- and concentration-dependent manners. The maximal glucose uptake was reached in the cells treated with APS (400 μg/mL) for 36 h. The APS-stimulated glucose uptake was significantly attenuated by pretreatment with Compound C, a selective AMPK inhibitor or in the cells overexpressing AS160-4P. Treatment of L6 myotubes with APS strongly promoted the activation of AMPK. We further demonstrated that either Ca^{2+}/calmodulin-dependent protein kinase kinase β (CaMKKβ) or liver kinase B1 (LKB1) mediated APS-induced activation of AMPK in L6 myotubes, and the increased cellular AMP: ATP ratio was also involved. Treatment of L6 myotubes with APS robustly enhanced the phosphorylation of AS160, which was significantly attenuated by pretreatment with Compound C.
Conclusion: Our results demonstrate that APS stimulates glucose uptake in L6 myotubes through the AMP-AMPK-AS160 pathway, which may contribute to its hypoglycemic effect.

Keywords: Astragalus polysaccharide; L6 myotubes; glucose uptake; AMP; AMPK; AS160; CaMKKβ; LKB1; type 2 diabetes mellitus

Acta Pharmacologica Sinica (2013) 34: 137–145; doi: 10.1038/aps.2012.133; published online 29 Oct 2012

Introduction

Type 2 diabetes mellitus (T2DM) is one of the fastest growing public health problems. The main defect due to this disease is impaired glucose homeostasis partly caused by insulin resistance. Glucose homeostasis is maintained when glucose production and utilization are in balance. Skeletal muscle, the main site for glucose disposal[1], displays decreased glucose uptake when insulin resistance occurs in T2DM patients[2, 3].

In addition to the classical insulin signaling pathway, glucose disposal in skeletal muscle is regulated by the AMP-activated protein kinase (AMPK) signaling pathway[4]. AMPK, a heterotrimeric protein kinase comprising a catalytic α-subunit and regulatory β- and γ-subunits[5], is activated by phosphorylation at the Thr172 residue of AMPKα, which is mediated by one or more upstream kinases. In addition, AMPK is allosterically activated by AMP[6, 7]. Once activated, AMPK switches on energy-generating pathways such as glucose transport. This finding has led to the concept that AMPK is a potential therapeutic drug target in situations of insulin resistance. Biguanides and thiazolidinediones, two classic antidiabetic drugs, have been used to treat T2DM patients due (at least in part) to their abilities to activate AMPK[8].

Activation of AMPK has been involved in the regulation of glucose uptake[9]; however, the signaling molecules connecting these events are still unknown. Akt substrate of 160 kDa (AS160; also known as TBC1D4) has been thought to be a key molecule linking the insulin and AMPK signaling pathways to glucose transporter 4 (GLUT4) translocation and subsequent glucose uptake in skeletal muscle[10]. AS160 has a Rab GTPase-activating protein (GAP) domain that plays a critical

* To whom correspondence should be addressed.
E-mail jpoy@163.com
Received 2012-04-26 Accepted 2012-08-05

role in regulating vesicle formation, vesicle movement, and membrane fusion[11]. Phosphorylation of AS160 is suspected to exhibit impairments in its Rab GAP activity, which permits target Rabs to return to their active GTP-bound forms and initiate GLUT4 exocytotic trafficking[12, 13]. AS160 phosphorylation is reduced in T2DM patients, which is accompanied by impaired GLUT4 translocation[14].

Many natural products have been used in traditional medicine to treat a variety of human diseases. *Astragalus membranaceus* Bunge (Huang Qi) is a popular traditional Chinese herb that has a long history of medicinal use in both Chinese and Western herbal medicine[15]. Astragalus polysaccharide (APS) was extracted from *Astragalus membranaceus* Bunge and identified as its main active component. Our previous studies have shown that APS has the ability to restore glucose homeostasis through the stimulation of glucose uptake in skeletal muscle cells[16]. To detail the mechanisms of this process, we examined the effects of APS on the AMPK signaling pathway in L6 myotubes. We hypothesized that APS might be capable of stimulating glucose uptake through the activation of AMPK and the phosphorylation of AS160 in L6 myotubes.

Materials and methods

Chemicals and reagents

APS was the goods of 'Astragalus polysaccharide for injection' (National authentication code Z20040086) purchased from Tianjin Cinorch Pharmaceutical Co, Ltd (Tianjin, China). High-glucose Dulbecco's modified Eagle's medium (HG-DMEM) was obtained from Invitrogen (Carlsbad, CA, USA). Fetal bovine serum (FBS) was purchased from Biochrom (Berlin, Germany), and 2-deoxy-[^{3}H]-D-glucose was obtained from Amersham Biosciences (Piscataway, NJ, USA). Rosiglitazone was obtained from Alexis (Lausen, Switzerland), and Compound C was purchased from Calbiochem (Darmstadt, Germany). Additionally, 5-aminoimidazole-4-carboxyamide-1-β-D-ribofuranoside (AICAR), STO-609, insulin, metformin, ionomycin, dimethyl sulfoxide (DMSO), and all other chemicals were obtained from Sigma-Aldrich (St Louis, MO, USA). Polyvinylidene difluoride (PVDF) membranes were purchased from Millipore (Billerica, MA, USA), and the bicinchoninic acid (BCA) protein assay kit was obtained from Pierce Biotechnology (Rockford, IL, USA). Enhanced chemiluminescence (ECL) reagents were purchased from Kirkegaard and Perry Laboratories (KPL, Gaithersburg, MD, USA).

Cell culture and differentiation

The L6 myoblast cell line was purchased from the American Type Culture Collection (Manassas, VA, USA). Following the manufacturer's protocol for cell culture and differentiation, L6 myoblasts were cultured in HG-DMEM supplemented with 10% (*v/v*) FBS, 100 U/mL penicillin, and 100 μg/mL streptomycin in a humidified atmosphere with 5% CO_2 at 37 °C.

For differentiation, cells were allowed to reach confluence, and the medium was switched to HG-DMEM containing 2% (*v/v*) FBS. During the subsequent 7-d period, the medium was changed every other day. All treatments in this study were initiated after differentiation had been successfully completed. Cells from passages 3–15 were used in the experiments, and undifferentiated cells were not allowed to grow to more than 60%–70% confluence.

2-Deoxy-[^{3}H]-D-glucose uptake assay

Glucose uptake was measured using the 2-deoxy-[^{3}H]-D-glucose method[17] with modifications as previously described[18]. Briefly, the assay was initiated by replacing the HG-DMEM with a glucose-free medium containing 50 μmol/L 2-deoxy-[^{3}H]-D-glucose (370 Bq/nmol). After incubation at 37 °C for 15 min, the cells were rinsed 3 times with ice-cold phosphate-buffered saline (PBS) and digested in 0.2 mol/L NaOH at 60 °C for 1 h. Liquid scintillation counting of the samples was performed to assess the amount of labeled glucose taken up by the cells. The net uptake of 2-deoxy-[^{3}H]-D-glucose was expressed in pmol·min^{-1}·mg^{-1} (protein)±SEM.

Western blot analysis

Cells were lysed in lysis buffer (20 mmol/L Tris, pH 7.5, 150 mmol/L NaCl, 1% Triton X-100, 2.5 mmol/L sodium pyrophosphate, 1 mmol/L β-glycerophosphate, 1 mmol/L EDTA, 1 mmol/L Na_3VO_4, 1 μg/mL leupeptin, and 1 mmol/L phenylmethylsulfonyl fluoride). The lysates were continuously stirred for 30 min before being centrifuged at 14 000×*g* for 10 min at 4 °C. The supernatants were assayed using the BCA protein assay kit to measure protein concentration. Cell lysates were separated by SDS-PAGE and transferred to PVDF membranes. The membranes were blocked with 5% bovine serum albumin (BSA) in TBST (Tris-buffered saline containing 0.1% Tween 20) for 2 h before incubation with primary antibodies overnight at 4 °C with gentle shaking. The primary antibodies included antibodies against AMPKα (Cell Signaling Technology), phospho-AMPKα (Thr172) (Millipore), acetyl-CoA carboxylase (ACC) (Millipore), phospho-ACC (Ser79) (Millipore), liver kinase B1 (LKB1) (Cell Signaling Technology), Myc-Tag (Cell Signaling Technology), AS160 (Millipore), phospho-(Ser/Thr) Akt substrate (Cell Signaling Technology), and β-Actin (Santa Cruz Biotechnology). After 3 washes (10 min/wash) with TBST, the membranes were incubated with a horseradish peroxidase (HRP)-conjugated secondary antibody (KPL) with gentle shaking at room temperature for 1 h. After the final incubation with the secondary antibody, the membranes were washed 3 times with TBST (10 min/wash). The proteins of interest were detected using ECL reagents.

AMPK activity assay

AMPK activity was measured using the HMRSAMSGLHLVKRR (SAMS) peptide as previously described[19]. Briefly, 200 μg of protein from each sample was prepared in triplicate and mixed with 500 μL of IP buffer (lysis buffer plus 1 mmol/L dithiothreitol). AMPK was immunoprecipitated by an incubation with an anti-AMPKα antibody prebound to protein A/G-agarose (Santa Cruz Biotechnology) at 4 °C for 2 h. The beads were collected after centrifugation at 14 000×*g* for 1 min and washed once with IP buffer and twice with

10×reaction buffer (400 mmol/L HEPES, pH 7.4, 50 mmol/L $MgCl_2$, 800 mmol/L NaCl, and 1 mmol/L dithiothreitol). Following the washes, 50 μL of a reaction mixture containing 5 μL of reaction buffer, 10 μL of ATP working stock (0.1 μL of 100 mmol/L ATP, 1 μL of [^{32}P]ATP, and 8.9 μL of H_2O), 10 μL of SAMS peptide (1 g/L), and 25 μL of H_2O was incubated with the beads for 10 min at 37 °C. The supernatants were spotted onto P81 Whatman filter papers, and the free [^{32}P]ATP was subsequently removed by washing the filter papers with 1% phosphoric acid 4–5 times. After the washes, the filter papers were quickly dried, and the radioactivity was measured using a liquid scintillation counter.

Adenine nucleotide extraction and measurement

The ATP, ADP, and AMP contents were measured by high-performance liquid chromatography (HPLC, Dionex Corporation, Sunnyvale, CA, USA) as previously described[20] with some modifications. Briefly, after treatment with different reagents, the cells were rinsed with PBS and digested with trypsin. Total cell numbers were counted before the cells were collected by centrifugation at 1000×*g* for 3 min. The cell pellets were resuspended in 150 μL of ice-cold perchloric acid (4% *v/v*) and incubated on ice for 30 min. After incubation, the cell lysates were neutralized with 2 mol/L KOH and centrifuged at 13 000×*g* at 4 °C for 10 min to remove the precipitated $KClO_4$. After passage through a 0.22-μm filter, the supernatants were aliquoted and stored at -80 °C.

The adenine nucleotide contents were determined using HPLC with a chromatography column (Phenomenex Luna C18 100A, 250×4.60 mm, 5 μm). Mobile phase A was phosphate buffer (50 mmol/L potassium dihydrogen orthophosphate, 50 mmol/L dipotassium hydrogen orthophosphate, pH 7.0, and 1 mmol/L EDTA), and mobile phase B was methyl hydrate. The adenine nucleotides were assayed spectrophotometrically at 259 nm and eluted after 15 min of isocratic elution at a flow rate of 1.0 mL/min. The HPLC peaks were identified and quantified by comparing the retention times and integrated peak areas with known external standards.

Plasmid DNA extraction and transient transfection

The cDNAs encoding AS160 were kindly provided by Dr Laurie J GOODYEAR (Joslin Diabetes Center, Boston, MA, USA) after we had obtained permission from the Kazusa DNA Research Institute (Kisarazu, Chiba, Japan). After signing a Material Transfer Agreement (MTA) with Dr Jun-ichi MIYAZAKI (Osaka University Medical School, Osaka, Japan), we obtained the pCAGGS vector from Dr Laurie J GOODYEAR. The wild-type AS160 (AS160-WT) DNA and 4P mutant AS160 (AS160-4P) DNA constructs have been previously characterized[21]. The accuracy of the DNA sequences was confirmed using the high-throughput DNA sequencing service provided by Invitrogen. Plasmid DNAs were amplified in *Escherichia coli* TOP10 cells (Invitrogen) and purified using an endotoxin-free Plasmid Midi Kit (Omega). For transient transfections, 8 μg of DNA were used per 6-cm dish along with 20 μL of Lipofectamine 2000 (Invitrogen) according to the manufacturer's protocol.

Statistical analysis

Data are expressed as the mean±SEM. Differences were determined by an analysis of variance (ANOVA) followed by Tukey's test. A level of $P<0.05$ was considered to be statistically significant.

Results

APS stimulated glucose uptake in time- and concentration-dependent manners

L6 myotubes were treated with 400 μg/mL APS for 6 to 48 h. As shown in Figure 1A, APS exposure increased glucose uptake in a time-dependent manner ($P<0.05$). Furthermore, the increased glucose uptake mediated by APS was concentration-dependent. APS increased glucose uptake when administered at a concentration of 100 μg/mL and induced maximal glucose uptake at 400 μg/mL (Figure 1B, $P<0.05$). Because 400 μg/mL APS resulted in an optimal increase of glucose uptake at 24 h, we used this concentration of APS along with a 24-h incubation period for all subsequent experiments.

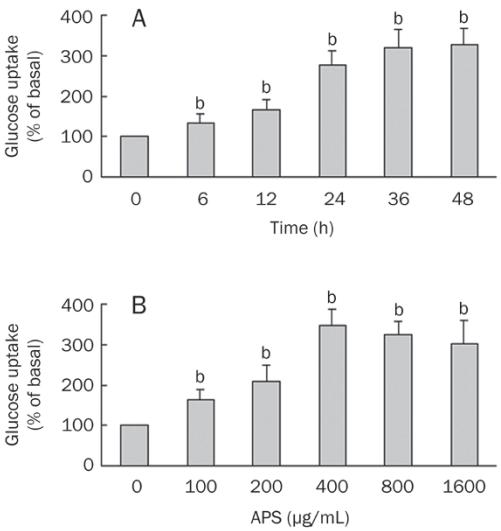

Figure 1. APS stimulated glucose uptake in time- and concentration-dependent manners. (A) L6 myotubes were serum-starved overnight and incubated with 400 μg/mL APS for various time periods up to 48 h. (B) L6 myotubes were serum-starved overnight and incubated for 24 h with increasing concentrations of APS. Mean±SEM. $n=5$. $^bP<0.05$ *vs* basal group.

APS stimulated the activation of AMPK and the phosphorylation of AS160

The signaling pathways triggered by APS were explored by Western blot analysis. APS increased the phosphorylation of AMPK-Thr172 (Figure 2A, $P<0.05$), which indicated an elevation in AMPK activity. Meanwhile, AMPK activation by APS was further confirmed by increased phosphorylation of ACC-Ser79, a direct substrate of AMPK (Figure 2A, $P<0.05$). In

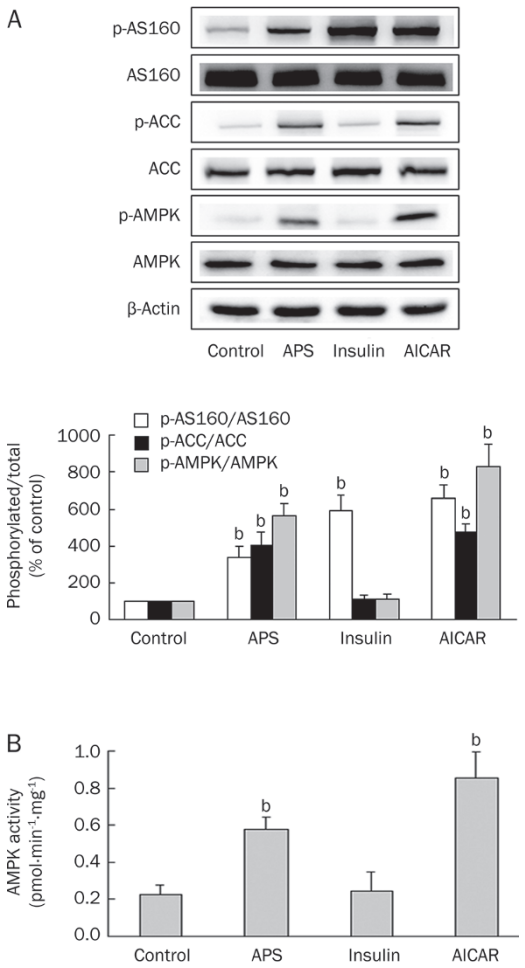

Figure 2. APS increased the activation of AMPK and the phosphorylation of AS160. L6 myotubes were incubated with different treatments (400 μg/mL APS for 24 h, 1 μmol/L insulin for 30 min, or 0.5 mmol/L AICAR for 30 min) before Western blot analysis and AMPK activity assay were performed. (A) Representative immunoblots show the effect of APS on the phosphorylation of AS160, ACC, and AMPK in L6 myotubes. The histogram shows the ratio of phosphorylated protein to total protein, and the data are expressed as a percentage of the response to control. (B) AMPK activity was assayed using the SAMS peptide. Results are plotted as pmol of phosphate incorporated into peptide per min per mg of total protein. Mean±SEM. n=5. ^bP<0.05 *vs* control group.

addition, APS augmented the activity of AMPK, which was determined by the phosphorylation of the SAMS peptide using [^{32}P]ATP assays (Figure 2B, P<0.05).

As shown in Figure 2A, an increase in AS160 phosphorylation was also observed in APS-treated L6 myotubes (P<0.05). In comparison, the phosphorylation of AS160, but not that of AMPK and ACC, was considerably increased in insulin-treated cells (P<0.05). AICAR, a well-known AMPK activator, robustly stimulated the phosphorylation of AS160 as well as that of AMPK and ACC (P<0.05).

Role of CaMKKβ and LKB1 in APS-induced AMPK activation

Ca^{2+}/calmodulin-dependent protein kinase kinase β (CaMKKβ) and LKB1 are two upstream AMPK kinases (AMPKKs). To evaluate whether either of these kinases is involved in the activation of AMPK by APS, we investigated the effect of STO-609, a selective inhibitor for CaMKKβ, on the activation of AMPK by APS in L6 myotubes. Exposure to ionomycin, a Ca^{2+} ionophore, stimulated the phosphorylation of AMPK and ACC in L6 myotubes, and the stimulatory effect was abrogated by STO-609 (Figure 3A, P<0.05). However, incubation with STO-609 did not abolish the enhanced phosphorylation of AMPK and ACC by APS in L6 myotubes (Figure 3A, P>0.05), which suggested that CaMKKβ might not be the major AMPK kinase in APS-induced AMPK activation. To explore the role that LKB1 plays in the activation of AMPK by APS, HeLa cells lacking LKB1 were used (Figure 3B). APS caused a significant increase in the phosphorylation of AMPK and ACC in HeLa cells (Figure 3C, P<0.05), indicating that LKB1 might not be the major AMPK kinase involved in APS-induced AMPK activation. Notably, incubation of HeLa cells with STO-609 abrogated the activation of AMPK by APS, ionomycin, and AICAR (Figure 3C, P<0.05).

APS increased the cellular AMP:ATP ratio

The above results demonstrate that alternate pathways leading to APS-induced AMPK activation may exist. Increases in AMP levels can induce AMPK activation[22]. To investigate the possibility that AMP participates in APS-induced AMPK activation, we measured the adenine nucleotide levels in L6 myotubes subjected to different AMPK-activating treatments. As shown in Figure 4 and Supplementary Table 1, incubation with APS caused marked increases in the levels of AMP and the calculated AMP:ATP ratio compared with untreated control cells (P<0.05). Similar increases were also observed in the treatment of L6 myotubes with rosiglitazone (P<0.05). Metformin increased the cellular AMP levels (P<0.05), but no difference in the calculated AMP:ATP ratio was observed compared with untreated control cells (P>0.05).

Increase in glucose uptake by APS was AMPK-dependent

AMPK has been previously demonstrated to increase glucose uptake in skeletal muscle in an insulin-independent manner[4]. To explore the possibility that AMPK is involved in APS-stimulated glucose uptake, we examined the role of Compound C, a selective AMPK inhibitor, on glucose uptake mediated by APS in L6 myotubes. As shown in Figure 5A, Compound C did not affect insulin-stimulated glucose uptake (P>0.05). However, Compound C reduced APS-stimulated glucose uptake (P<0.05), indicating that AMPK played a role in the effect of APS on glucose uptake. A similar attenuation was observed following incubation with AICAR (P<0.05).

Because incubation with the CaMKKβ inhibitor STO-609 did not abolish the enhanced phosphorylation of AMPK by APS in L6 myotubes (Figure 3A), we reasoned that APS-stimulated glucose uptake should not be inhibited by this inhibitor. Indeed, STO-609 did not significantly inhibit APS-stimulated glucose uptake in L6 myotubes (Figure 5B, P>0.05). Similar effects were also observed in the treatment of L6 myotubes

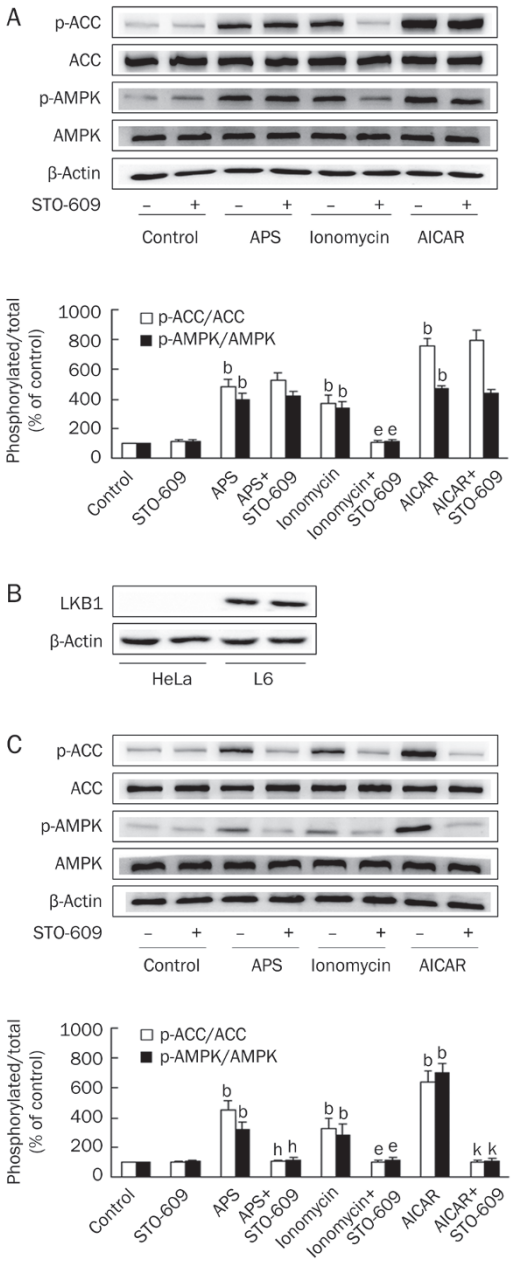

Figure 3. Effects of LKB1 deficiency and CaMKKβ inhibition on APS-induced AMPK activation. (A) L6 myotubes were treated with 400 μg/mL APS for 24 h, 1 μmol/L ionomycin for 30 min, or 0.5 mmol/L AICAR for 30 min after preincubation in the presence or absence of 10 μg/mL STO-609 for 1 h. (B) LKB1 expression in HeLa cells and L6 myotubes. (C) HeLa cells were incubated with 400 μg/mL APS for 24 h, 1 μmol/L ionomycin for 30 min, or 0.5 mmol/L AICAR for 30 min with or without preincubation with STO-609 (10 μg/mL) for 1 h. Histograms show the ratio of phosphorylated protein to total protein. Mean±SEM. n=5. ^{b}P<0.05 *vs* control group. ^{e}P<0.05 *vs* ionomycin group. ^{h}P<0.05 *vs* APS group. ^{k}P<0.05 *vs* AICAR group.

with insulin or AICAR (Figure 5B, P>0.05).

Overexpression of AS160 in transfected L6 myoblasts

The expression of recombinant AS160-WT and AS160-4P isoforms was accomplished using our gene transfer approach. Lysates from transfected cells were immunoblotted with antibodies against the Myc epitope tag and the carboxyl terminus of rat AS160 (amino acids 1178-1189) (Figure 5C). Notably, the AS160 antibody detected endogenous rat AS160 (rAS160, lower band) and exogenous Myc-tagged human AS160 (hAS160, upper band). Both bands were used in densitometry quantifications. On the basis of the histogram in Figure 5C, approximately equal amounts of the wild-type and mutant forms of Myc-tagged human AS160 were expressed, and the transfected cells expressed approximately 7 times more Myc-tagged human AS160 than endogenous rat AS160 (P<0.01). In contrast, there were no significant changes in the phosphorylation of ACC and AMPK in L6 myoblasts transfected with empty pCAGGS vector, AS160-WT, or AS160-4P (Figure 5D, P>0.05).

APS increased glucose uptake through AS160

In skeletal muscle, the phosphorylation and deactivation of AS160 are involved in the regulation of AMPK on glucose uptake, which is able to facilitate the translocation of GLUT4 vesicles to the plasma membrane by a relief of inhibition mechanism[23, 24]. In L6 myotubes, APS increased glucose uptake (Figure 1) and AS160 phosphorylation (Figure 2A). Hence, we further attempted to determine whether APS-stimulated glucose uptake was mediated by AS160. AS160 is phosphorylated at several sites, and Ser318, Ser588, Thr642, and Ser751 are considered to be the most important sites for AS160-mediated regulation of glucose uptake[21]. Therefore, we expressed AS160-WT and AS160-4P (containing 4 mutations, ie, S318A, S588A, T642A, and S751A) constructs in L6 myoblasts by transient transfection. As shown in Figure 5E, L6 myoblasts overexpressing AS160-4P exhibited a robust impairment in APS-stimulated glucose uptake relative to myoblasts expressing AS160-WT (P<0.05). Similar attenuations were observed following incubation with insulin or AICAR (P<0.05). In accordance with these results, AS160 is a key molecule in APS-stimulated glucose uptake.

Phosphorylation of AS160 by APS was AMPK-dependent

AS160 has been reported to be an AMPK substrate *in vitro*, and the phosphorylation of AS160 is regulated by AMPK in the isolated extensor digitorum longus muscle[24]. To determine whether AMPK is involved in APS-stimulated AS160 phosphorylation, L6 myotubes were pretreated with Compound C, a selective AMPK inhibitor, prior to Western blot analysis. As indicated in Figure 6, Compound C attenuated the APS- and AICAR-mediated increase in AS160 phosphorylation as well as phosphorylation of AMPK-Thr172 and ACC-Ser79 (P<0.05). However, insulin-stimulated AS160 phosphorylation was not inhibited by Compound C (P>0.05). These results suggest that APS-stimulated AS160 phosphorylation is AMPK-dependent.

Discussion

First, we show that APS stimulates glucose uptake in L6 myotubes through AMPK, which has been previously reported

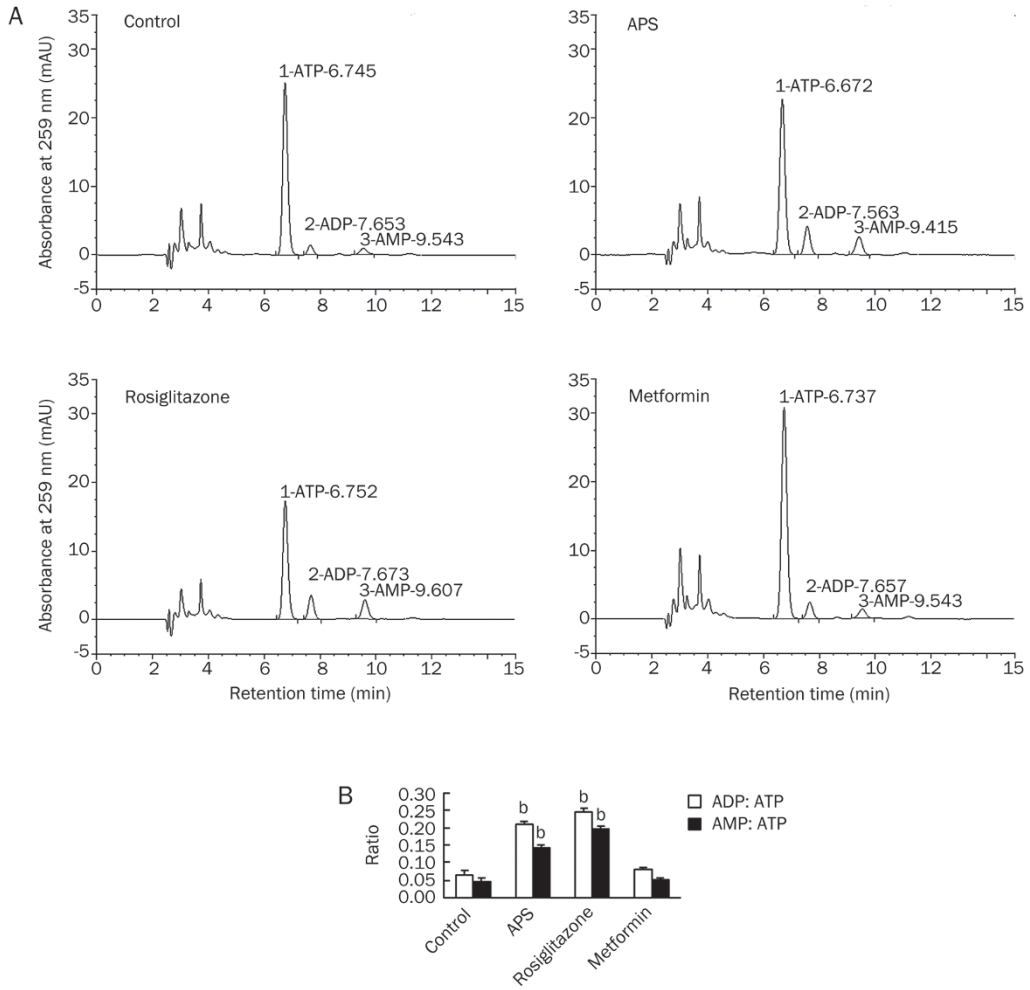

Figure 4. APS increased the cellular AMP: ATP ratio. L6 myotubes were incubated with different treatments (400 μg/mL APS for 24 h, 200 μmol/L rosiglitazone for 30 min, or 2 mmol/L metformin for 3 h) before adenine nucleotides were extracted and analyzed using HPLC. (A) In each case, a representative trace is shown. The positions at which ATP, ADP, and AMP standards elute are indicated on each trace. (B) The histogram shows the ratios of ADP: ATP and AMP: ATP. Mean±SEM. n=5. $^bP<0.05$ *vs* control group.

in our experiments using animal models of T2DM to test this hypothesis[16]. These results highlight the importance of AMPK as a promising antidiabetic drug target. Second, we determine that AMP is the major contributor to APS-induced AMPK activation in L6 myotubes, which is consistent with other reports showing that AMP may regulate AMPK activation through the inhibition of AMPK phosphatase under conditions of metabolic stress[25]. Finally, we provide evidence that APS strongly increases AS160 phosphorylation, which mediates APS-stimulated glucose uptake in L6 myotubes. These results suggest that AS160 participates in the hypoglycemic effect of APS.

AMPK is believed to play a central role in the energy homeostasis system, especially in reports concerning the pathophysiology and therapy of T2DM. Following activation by exercise or pharmacological agents, AMPK could reverse the abnormal energy processes associated with T2DM[8]. These observations suggest that it is possible to treat T2DM patients with AMPK activators. In this study, we determined that APS activated AMPK in L6 myotubes and exhibited some important beneficial metabolic effects in response to AMPK activation, including the phosphorylation of ACC and AS160.

There are two major signaling pathways that participate in glucose transport in skeletal muscle. One is the insulin signaling pathway, and the other is the AMPK signaling pathway[26]. Whether crosstalk exists between these two signaling pathways is still unclear. In this study, we showed that APS-stimulated glucose uptake was dependent on AMPK in L6 myotubes. In our previous study, we determined that the insulin signaling pathway was activated after treatment with APS[27]. These data suggest that both signaling pathways could be activated by APS. However, we could not conclude that intercommunication was occurring between these two signaling pathways in the presence of APS. Therefore, further studies are required to elucidate how these two signaling pathways collectively contribute to the hypoglycemic effect of APS.

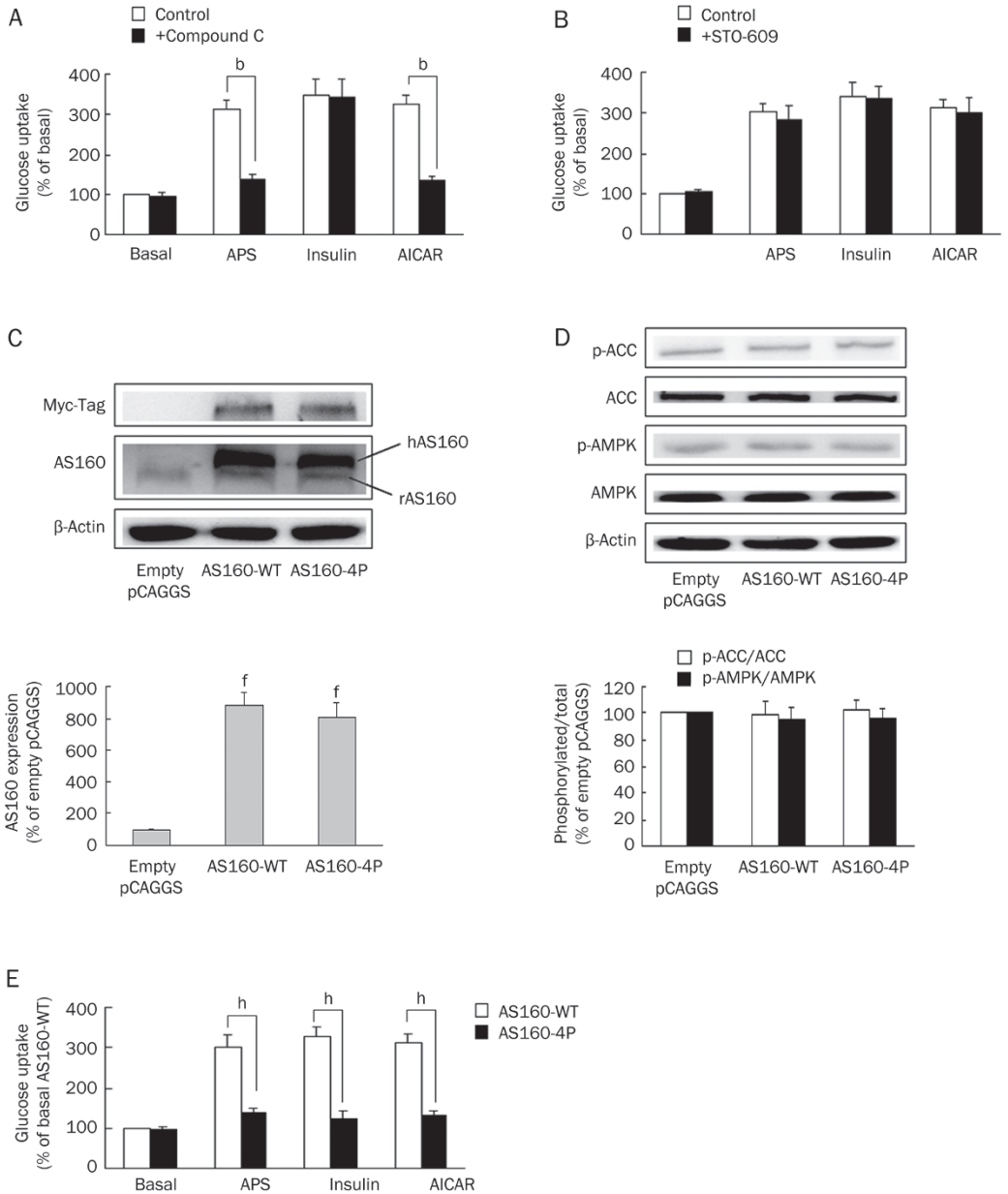

Figure 5. Effects of AMPK inhibition, CaMKKβ inhibition and AS160 mutant on APS-stimulated glucose uptake. (A) L6 myotubes were treated with 400 μg/mL APS for 24 h, 1 μmol/L insulin for 30 min, or 0.5 mmol/L AICAR for 30 min after preincubation in the presence or absence of 1 μmol/L Compound C for 30 min. (B) L6 myotubes were treated with 400 μg/mL APS for 24 h, 1 μmol/L insulin for 30 min, or 0.5 mmol/L AICAR for 30 min with or without preincubation with STO-609 (10 μg/mL) for 1 h. (C) Expression of AS160 in L6 myoblasts transfected with empty pCAGGS vector, AS160-WT, or AS160-4P. (D) Representative immunoblots show the effect of AS160 mutant on the phosphorylation of ACC and AMPK in L6 myoblasts. The histogram shows the ratio of phosphorylated protein to total protein, and the data are expressed as a percentage of the response to empty pCAGGS group. (E) Effect of AS160 mutant on APS- (400 μg/mL, 24 h), insulin- (1 μmol/L, 30 min), or AICAR- (0.5 mmol/L, 30 min) mediated glucose uptake in L6 myoblasts. Mean±SEM. n=5. ^{b}P<0.05 *vs* control group. ^{f}P<0.01 *vs* empty pCAGGS group. ^{h}P<0.05 *vs* AS160-WT group.

The name "AMP-activated protein kinase" comes from a study in which the activity of this kinase was shown to be regulated by AMP[28]. AMP augments the activity of AMPK in two possible ways. One mechanism is the induction of a conformational change in the γ subunit following binding to AMP, which can be activated by allosteric regulation[29]. The other mechanism is the inhibition of AMPK dephosphorylation by protein phosphatases[25, 30]. In cell-free systems, protein phosphatase-2A and protein phosphatase-2C (PP2A/PP2C) dephosphorylate AMPK at Thr172 after binding to the threonine residue of AMPK, and AMP could inhibit this reaction by preventing this binding, which could increase the activity of AMPK[25, 30, 31]. Therefore, AMP activates AMPK by causing allosteric activation of AMPK as well as by making AMPK a

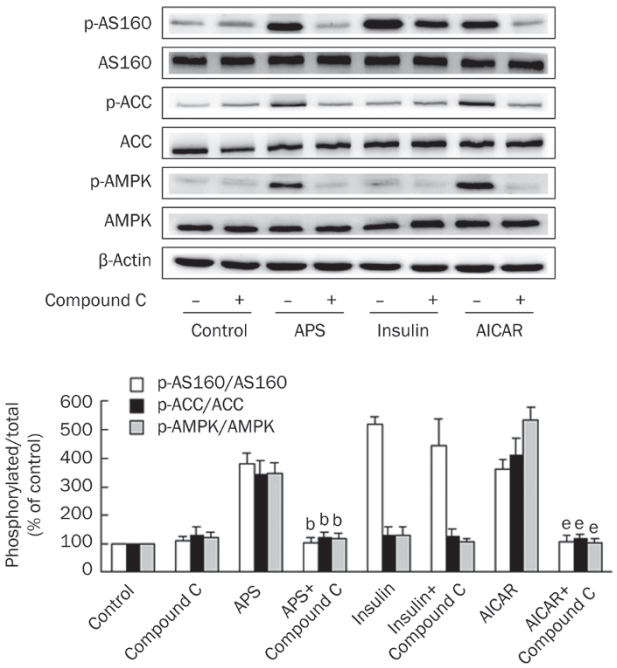

Figure 6. APS-stimulated AS160 phosphorylation was AMPK-dependent. L6 myotubes were preincubated with Compound C (1 μmol/L) for 30 min followed by treatment with APS (400 μg/mL, 24 h), insulin (1 μmol/L, 30 min), or AICAR (0.5 mmol/L, 30 min). The histogram shows the ratio of phosphorylated protein to total protein. Mean±SEM. n=5. ^{b}P<0.05 *vs* APS group. ^{e}P<0.05 *vs* AICAR group.

worse substrate for protein phosphatases. Here, we showed that APS increased the cellular AMP levels and the AMP:ATP ratio in L6 myotubes, which may provide a mechanistic explanation for the activation of AMPK by APS.

Other possible mechanisms involved in APS-induced AMPK activation were tested using HeLa cells (lacking LKB1) and the CaMKKβ inhibitor STO-609. We observed that the activation of AMPK in HeLa cells by APS was blocked by pretreatment with STO-609. However, we showed that STO-609 did not block the activation of AMPK by APS in the L6 myotubes that express LKB1 and CaMKKβ. These findings suggest that APS-induced AMPK activation can be mediated by either LKB1 or CaMKKβ. Additionally, we discovered that AMPK was activated in HeLa cells by AICAR, an adenosine analogue, and that this activation was abolished by STO-609. As discussed above, AMP, LKB1, and CaMKKβ may serve as upstream activators that mediate APS-induced AMPK activation.

In adult skeletal muscle, insulin, the AMPK activator AICAR, and contraction stimulate AS160 phosphorylation concomitant with glucose uptake[23, 32]. AS160 phosphorylation is induced by different signaling molecules due to various stimuli. In skeletal muscle, Akt mediates insulin-stimulated AS160 phosphorylation; AMPK induces AICAR-stimulated AS160 phosphorylation; and AMPK and to a lesser extent Akt regulate contraction-stimulated AS160 phosphorylation[24, 32]. Our present study demonstrated that APS could stimulate AS160 phosphorylation and that AMPK contributed to APS-stimulated AS160 phosphorylation. Whether Akt mediated this APS-stimulated AS160 phosphorylation was unresolved in this study. Therefore, in the future, it will be important to elucidate the role of Akt in APS-stimulated AS160 phosphorylation and glucose uptake.

To summarize, we demonstrate for the first time that APS enhances AS160 phosphorylation to stimulate glucose uptake in an AMPK-dependent manner, which supports the development of APS as a promising and potent candidate for the treatment of T2DM.

Acknowledgements

We are especially grateful to Dr Laurie J GOODYEAR (Joslin Diabetes Center, Boston, MA, USA), Dr Takahiro NAGASE (Kazusa DNA Research Institute, Chiba, Japan), and Dr Junichi MIYAZAKI (Osaka University Medical School, Osaka, Japan) for providing valuable materials.

This work was supported by the National Natural Science Foundation of China (No 30771023).

Author contribution

Jian LIU, Jing-fang ZHANG, and Jing-ping OU-YANG designed the research; Jian LIU, Jin-zhi LU, Ke SU, Si-tu YANG, and Lang BU performed the research and analyzed the data; De-ling ZHANG, Jing WANG, and Ye-min ZHANG contributed new analytical tools and reagents; Jian LIU drafted the manuscript; and Jing-fang ZHANG, Ke LI, Nian WANG, and Jing-ping OU-YANG revised the manuscript.

Supplementary information

Supplementary table is available at the Acta Pharmacologica Sinica website.

References

1 DeFronzo RA, Jacot E, Jequier E, Maeder E, Wahren J, Felber JP. The effect of insulin on the disposal of intravenous glucose. Results from indirect calorimetry and hepatic and femoral venous catheterization. Diabetes 1981; 30: 1000–7.

2 Dohm GL, Tapscott EB, Pories WJ, Dabbs DJ, Flickinger EG, Meelheim D, *et al*. An *in vitro* human muscle preparation suitable for metabolic studies. Decreased insulin stimulation of glucose transport in muscle from morbidly obese and diabetic subjects. J Clin Invest 1988; 82: 486–94.

3 DeFronzo RA, Bonadonna RC, Ferrannini E. Pathogenesis of NIDDM. A balanced overview. Diabetes Care 1992; 15: 318–68.

4 Misra P, Chakrabarti R. The role of AMP kinase in diabetes. Indian J Med Res 2007; 125: 389-98.

5 Hardie DG, Scott JW, Pan DA, Hudson ER. Management of cellular energy by the AMP-activated protein kinase system. FEBS Lett 2003; 546: 113–20.

6 Hawley SA, Davison M, Woods A, Davies SP, Beri RK, Carling D, *et al*. Characterization of the AMP-activated protein kinase kinase from rat liver and identification of threonine 172 as the major site at which it phosphorylates AMP-activated protein kinase. J Biol Chem 1996; 271: 27879–87.

7 Stein SC, Woods A, Jones NA, Davison MD, Carling D. The regulation of AMP-activated protein kinase by phosphorylation. Biochem J 2000; 345: 437-43.

8 Hardie DG. AMPK: a key regulator of energy balance in the single cell and the whole organism. Int J Obes (Lond) 2008; 32: S7–12.
9 Merrill GF, Kurth EJ, Hardie DG, Winder WW. AICA riboside increases AMP-activated protein kinase, fatty acid oxidation, and glucose uptake in rat muscle. Am J Physiol 1997; 273: E1107–12.
10 Sakamoto K, Holman GD. Emerging role for AS160/TBC1D4 and TBC1D1 in the regulation of GLUT4 traffic. Am J Physiol Endocrinol Metab 2008; 295: E29–37.
11 Zerial M, McBride H. Rab proteins as membrane organizers. Nat Rev Mol Cell Biol 2001; 2: 107–17.
12 Sano H, Eguez L, Teruel MN, Fukuda M, Chuang TD, Chavez JA, *et al*. Rab10, a target of the AS160 Rab GAP, is required for insulin-stimulated translocation of GLUT4 to the adipocyte plasma membrane. Cell Metab 2007; 5: 293–303.
13 Zeigerer A, McBrayer MK, McGraw TE. Insulin stimulation of GLUT4 exocytosis, but not its inhibition of endocytosis, is dependent on RabGAP AS160. Mol Biol Cell 2004; 15: 4406–15.
14 Karlsson HK, Zierath JR, Kane S, Krook A, Lienhard GE, Wallberg-Henriksson H. Insulin-stimulated phosphorylation of the Akt substrate AS160 is impaired in skeletal muscle of type 2 diabetic subjects. Diabetes 2005; 54: 1692–7.
15 Wang N, Zhang DL, Mao XQ, Zou F, Jin H, Ou-Yang JP. Astragalus polysaccharides decreased the expression of PTP1B through relieving ER stress induced activation of ATF6 in a rat model of type 2 diabetes. Mol Cell Endocrinol 2009; 307: 89–98.
16 Zou F, Mao XQ, Wang N, Liu J, Ou-Yang JP. Astragalus polysaccharides alleviates glucose toxicity and restores glucose homeostasis in diabetic states via activation of AMPK. Acta Pharmacol Sin 2009; 30: 1607–15.
17 Tanishita T, Shimizu Y, Minokoshi Y, Shimazu T. The beta3-adrenergic agonist BRL37344 increases glucose transport into L6 myocytes through a mechanism different from that of insulin. J Biochem 1997; 122: 90–5.
18 Hutchinson DS, Bengtsson T. alpha1A-adrenoceptors activate glucose uptake in L6 muscle cells through a phospholipase C-, phosphatidylinositol-3 kinase-, and atypical protein kinase C-dependent pathway. Endocrinology 2005; 146: 901–12.
19 Zou MH, Hou XY, Shi CM, Kirkpatick S, Liu F, Goldman MH, *et al*. Activation of 5′-AMP-activated kinase is mediated through c-Src and phosphoinositide 3-kinase activity during hypoxia-reoxygenation of bovine aortic endothelial cells. Role of peroxynitrite. J Biol Chem 2003; 278: 34003–10.
20 Hahn-Windgassen A, Nogueira V, Chen CC, Skeen JE, Sonenberg N, Hay N. Akt activates the mammalian target of rapamycin by regulating cellular ATP level and AMPK activity. J Biol Chem 2005; 280: 32081–9.
21 Sano H, Kane S, Sano E, Miinea CP, Asara JM, Lane WS, et al. Insulin-stimulated phosphorylation of a Rab GTPase-activating protein regulates GLUT4 translocation. J Biol Chem 2003; 278: 14599–602.
22 Hardie DG. Minireview: the AMP-activated protein kinase cascade: the key sensor of cellular energy status. Endocrinology 2003; 144: 5179–83.
23 Bruss MD, Arias EB, Lienhard GE, Cartee GD. Increased phosphorylation of Akt substrate of 160 kDa (AS160) in rat skeletal muscle in response to insulin or contractile activity. Diabetes 2005; 54: 41–50.
24 Treebak JT, Glund S, Deshmukh A, Klein DK, Long YC, Jensen TE, *et al*. AMPK-mediated AS160 phosphorylation in skeletal muscle is dependent on AMPK catalytic and regulatory subunits. Diabetes 2006; 55: 2051–8.
25 Suter M, Riek U, Tuerk R, Schlattner U, Wallimann T, Neumann D. Dissecting the role of 5′-AMP for allosteric stimulation, activation, and deactivation of AMP-activated protein kinase. J Biol Chem 2006; 281: 32207–16.
26 Russell RR 3rd, Bergeron R, Shulman GI, Young LH. Translocation of myocardial GLUT-4 and increased glucose uptake through activation of AMPK by AICAR. Am J Physiol 1999; 277: H643–9.
27 Wu Y, Ou-Yang JP, Wu K, Wang Y, Zhou YF, Wen CY. Hypoglycemic effect of Astragalus polysaccharide and its effect on PTP1B. Acta Pharmacol Sin 2005; 26: 345–52.
28 Yeh LA, Lee KH, Kim KH. Regulation of rat liver acetyl-CoA carboxylase. Regulation of phosphorylation and inactivation of acetyl-CoA carboxylase by the adenylate energy charge. J Biol Chem 1980; 255: 2308–14.
29 Scott JW, Hawley SA, Green KA, Anis M, Stewart G, Scullion GA, *et al*. CBS domains form energy-sensing modules whose binding of adenosine ligands is disrupted by disease mutations. J Clin Invest 2004; 113: 274–84.
30 Davies SP, Helps NR, Cohen PT, Hardie DG. 5′-AMP inhibits dephosphorylation, as well as promoting phosphorylation, of the AMP-activated protein kinase. Studies using bacterially expressed human protein phosphatase-2C alpha and native bovine protein phosphatase-2AC. FEBS Lett 1995; 377: 421–5.
31 Wu Y, Song P, Xu J, Zhang M, Zou MH. Activation of protein phosphatase 2A by palmitate inhibits AMP-activated protein kinase. J Biol Chem 2007; 282: 9777–88.
32 Kramer HF, Witczak CA, Fujii N, Jessen N, Taylor EB, Arnolds DE, *et al*. Distinct signals regulate AS160 phosphorylation in response to insulin, AICAR, and contraction in mouse skeletal muscle. Diabetes 2006; 55: 2067–76.